THE UNIVERSITY OF

WARWICK

Original citation:
Permanent WRAP url:
http://wrap.warwick.ac.uk/67813

warwickpublicationswrap

highlight your research

http://wrap.warwick.ac.uk/

Quad-Barrel Multifunctional Electrochemical and Ion Conductance Probe for Voltammetric Analysis and Imaging

Binoy Paulose Nadappuram, Kim McKelvey, Joshua C. Byers, Aleix G. Güell, Alex W. Colburn, Robert A. Lazenby, Patrick R. Unwin*

Department of Chemistry, University of Warwick, Coventry, U.K. CV4 7AL.

*P.R.Unwin@warwick.ac.uk

1

ABSTRACT

The fabrication and use of a multifunctional electrochemical probe incorporating two independent carbon working electrodes and two electrolyte-filled barrels, equipped with quasi-reference counter electrodes (QRCEs), in the end of a tapered micron-scale pipet is described. This 'quad-probe' (4-channel probe) was fabricated by depositing carbon pyrolytically into two diagonally opposite barrels of a laser-pulled quartz quadruple-barrelled pipet. After filling the open channels with electrolyte solution, a meniscus forms at the end of the probe and covers the two working electrodes. The two carbon electrodes can be used to drive local electrochemical reactions within the meniscus while a bias between the QRCEs in the electrolyte channels provides an ion conductance signal that is used to control and position the meniscus on a surface of interest. When brought into contact with a surface, localized high resolution amperometric imaging can be achieved with the two carbon working electrodes with a spatial resolution defined by the meniscus contact area. The substrate can be an insulating material or (semi)conductor, but herein we focus mainly on conducting substrates that can be connected as a third working electrode. Studies using both aqueous and ionic liquid electrolytes in the probe, together with gold and individual single walled carbon nanotube samples, demonstrate the utility of the technique. Substrate generation-dual tip collection measurements are shown to be characterized by high collection efficiencies (approaching 100%). This hybrid configuration of scanning electrochemical microscopy (SECM) and scanning electrochemical cell microscopy (SECCM) should be powerful for future applications in electrode mapping, as well as in studies of insulating materials as demonstrated by transient spot redox-titration measurements at an electrostatically charged Teflon surface and at a pristine calcite surface, where a functionalized probe is used to follow the immediate pH change due to dissolution.

INTRODUCTION

The localized investigation of interfaces is of importance towards understanding the behavior of heterogeneous surfaces such as electrodes, catalysts and biological membranes.[1-5] Furthermore, since such interfaces are often (electro)chemically dynamic, the ability to probe reactive fluxes locally is particularly beneficial for developing microscopic models of interfacial reactivity. In this context, electrochemical scanning probe microscopy techniques, especially scanning electrochemical microscopy (SECM)[6-8] and scanning droplet-based electrochemical techniques,[9-11] have revealed considerable quantitative information on surface and interfacial processes.

SECM employs a mobile ultramicroelectrode (UME) placed close to a sample bathed in solution, the response of which depends on the (electro)chemical properties and topography of the sample.[12-14] In contrast, scanning droplet electrochemical techniques use a liquid droplet formed at the end of a probe to assemble an electrochemical cell on a sample surface, and hence confine electrochemical reactions to the contact area between the droplet and the surface.[15,16] Probes of this type have tended to have large footprints and have been used for the characterization of a variety of substrates and surface properties.[17,18] More recently, scanning droplet techniques have evolved to allow the imaging of electrochemical activity with higher spatial resolution.[19]

Among scanning droplet techniques, scanning electrochemical cell microscopy (SECCM) has been developed by us as a means of achieving high control over meniscus contact with a surface.[20] In this approach, a tapered theta pipet filled with electrolyte solution serves as the probe and the ion current measured between the quasi-reference counter electrodes (QRCEs), one in each of the two barrels, provides a feedback signal for

positioning the probe close to the surface, making it possible to maintain a constant probe-surface distance irrespective of the surface topography.[17] This type of technique has been employed to deposit biomolecules[21] and reagents on surfaces[22,23] and for simultaneous electrochemical and topography imaging of surfaces in aqueous[17,24,25] and non-aqueous environments.[5]

In droplet-based techniques the sample surface wetted by the meniscus can be an insulator or, if a (semi)conductor, can act as a working electrode where the electrochemical activity can be measured.[9,20] However, by incorporating additional working electrodes into the end of the probe it is possible to enhance the capability of these types of techniques. Fountain pen probes,[26] incorporating a microfluidic channel with integrated working and counter/reference electrodes, employ just such a scheme. Microfluidic push-pull probes[27,28] that incorporate a working electrode into a droplet at the end of a probe, have also been reported for performing electrochemical measurements in a constantly renewed electrolyte droplet. At present, such probes operate with quite large footprints to enable a large area of sample to be investigated.[17]

Herein, we present a simple and quick method for fabricating a new type of probe comprising two open barrels that are filled with electrolyte and equipped with QRCEs and two carbon working electrodes. We call this a *quad-probe*, and used it for high resolution electrochemical characterization of surfaces. The probe combines the merits of SECM and SECCM by creating a droplet cell incorporating two independent working electrodes directly into a micron-scale droplet which can be moved and positioned on a substrate enabling multifunctional surface imaging and the localized investigation of processes at surfaces and interfaces. The capability of this technique for amperometric surface imaging is demonstrated by mapping the surface electrochemical activity of a gold band electrode on glass and an individual single-walled carbon nanotube (SWNT) on an insulating surface. In the latter case,

we employed a room temperature ionic liquid (RTIL) as the supporting electrolyte in the quad-probe to demonstrate the wide range of electrolytes open to study. In addition, the versatility of this quad-probe was further demonstrated by employing them to investigate a redox reaction at an insulating surface charged by contact electrification and by monitoring the pH change accompanying the dissolution of calcite.

EXPERIMENTAL SECTION

Details of standard materials, reagents, instrumentation and sample preparation methods are given in Supporting Information (Sections 1, 2 and 3). Herein, we give details relating to the quad-probe fabrication and applications.

Quad-probe fabrication. The quad-probes were fabricated from quartz quadruple-barrelled capillaries (MBT-015-062-4Q, Friedrich & Dimmock, Inc.), pulled to a sharp point by a laser puller (P-2000, Sutter Instruments) using a custom-developed two line program (Line 1:HEAT-925, FILAMENT-4, VELOCITY-40, DELAY-130, PULL-40; Line 2:HEAT-875, FILAMENT-4, VELOCITY-60, DELAY-126, PULL-35). Two diagonally opposite barrels were filled with carbon to form the electrodes by adapting a carbon electrode fabrication process described previously.[29-31] Briefly, the top ends of two diagonally opposite barrels were closed by using 'Blu-Tack' (Bostik, UK) and butane was passed through the other two barrels, via tubing, with the end held under an argon atmosphere. The tip of the pipet was heated with a butane torch, for 35 s, to deposit carbon pyrolytically from the butane, thus forming the electrodes, as illustrated in Figure 1A.

Field-emission scanning electron microscopy (FE-SEM, Supra 55-VP, Zeiss) of a typical quad-probe is shown in Figure 1B. A range of probe sizes, between 200 nm and 10

μm across each barrel, were easily fabricated by changing the laser pulling parameters during fabrication, but herein we focus on probes with a size of ca. 1 μm across each barrel.

At this stage, the probes were useable but some were further optimized by focused ion beam (FIB) cutting, which is a powerful method for tailoring carbon nanoelectrodes.[32] We used FIB-SEM (JEOL 4500, JEOL), at an accelerating voltage of 5 kV, with gallium ions (Ga^+). Figure 1B shows the lateral view of a typical quad-probe before and after FIB cutting. An electrical connection was established to each carbon electrode by inserting a copper wire through the top end of the pipet barrel to make a back contact. The open barrels were filled with the solution of interest and a AgCl-coated Ag wire, acting as a QRCE, was inserted into each. A liquid meniscus naturally formed at the end of the probe, covering the carbon electrodes to make a multifunctional droplet-based electrochemical cell.

Electrochemical configuration. A four or five electrode configuration was used, comprising the two carbon working electrodes in the probe, two Ag/AgCl QRCEs in the open (electrolyte-filled) barrels of the probe and, when in contact with a substrate electrode, this was a third working electrode. This configuration is illustrated in Figure 1D. The potential was controlled with respect to ground (V_{1-4} in Figure 1D) and current was measured (i_{1-4} in Figure 1D) at each electrode in the probe independently using a custom-built 'quadpotentiostat'. For transient pH measurements, a slightly different electrode configuration was used, where the potential was controlled with respect to one of the QRCEs in the open barrel which was held at 0 V with respect to ground and the open circuit potential at the pH electrode (with respect to the QRCE held at 0 V) was measured using a custom-build voltage follower.[31] An additional custom-built current to voltage convertor was employed at the substrate to measure the substrate current (i_5 in Figure 1D). The potential of the substrate was also controlled with respect to ground (V_5) and could be defined with respect to the QRCEs.

Electrochemical imaging. To position the probe close to the substrate, an ion current based feedback control scheme was used.[20] Briefly, a 100 mV bias was applied between the QRCEs to induce an ion current between the open barrels of the probe. The probe was oscillated (60 nm peak-peak amplitude, 280 Hz frequency) normal to the surface, generating an alternating current (i_{AC}) when the meniscus was in contact with the sample. This i_{AC} was measured via the lock-in amplifier and the magnitude of i_{AC} was used as a feedback signal to detect contact between the liquid meniscus and the surface, and to control the separation between the tip of the probe and the surface as in conventional SECCM.[20] Two-dimensional electrochemical images of the substrate surface were constructed from a series of line scans, during which the probe was moved laterally, with i_{AC} magnitude feedback control that maintained a constant tip-substrate separation, via a feedback loop. A similar feedback method was employed for electrostatic charge measurements at Teflon (see Supporting Information, Section 6) and local pH measurements at calcite (see Supporting Information, Section 7).

RESULTS AND DISCUSSIONS

Fabrication and characterization of quad-probes. A typical quad-probe (Figure 1C) consists of four quadrant shaped sectors, of which two diagonally opposite sectors were filled with carbon to form the working electrodes (top and bottom in Figure 1B) and the other two sectors were left open (left and right in Figure 1B). The size of the sectors and the thickness of the side walls were dependent on the laser pulling parameters employed. Herein, sectors with characteristic dimensions ca. 1 µm were used.

When the two open barrels of the quad-probes were filled with solution, a liquid meniscus (droplet) was formed at the end of the probe. This meniscus covered both the carbon electrodes forming a small electrochemical droplet cell. With the probes in air (Figure 2A), linear sweep voltammograms (LSVs) of individual carbon electrodes within quad-

probes were recorded for the one-electron oxidation of ferrocenylmethyl trimethylammonium (FcTMA$^+$) to FcTMA^{2+}. The potential, V_1 for electrode 1 or V_2 for electrode 2 (see Figure 1D), was swept at 50 mV/s over defined values with respect to ground, (with the other working electrode unconnected) while the potential of the QRCEs was held at ground. Responses of the two electrodes in a typical probe are shown as dashed lines in Figure 2B. As expected of a microscale electrode for moderate timescales,[33] the LSVs at each electrode shows a sigmoidal response. The magnitude of the limiting current for each electrode was slightly different, because the sizes and positions of the electrodes are different, which is common for probes fabricated by this type of method.[30] The magnitude of the limiting current depends on the mass transport to the electrode which, in the droplet configuration with only one active working electrode, is limited to diffusion of the electroactive species (FcTMA$^+$) down the two open barrels of the probe.[34]

Next, the same probe was used in air in a generation/collection (G/C) mode using FcTMA$^{+/2+}$ as the redox couple (Figure 2A). For this, the potential of one of the carbon electrodes (designated as the generator electrode) was swept for the one-electron oxidation of FcTMA$^+$ to FcTMA^{2+} (from $V_1 = 0$ V to 0.6 V with respect to ground) while keeping the potential of the other electrode (designated as the collector electrode) at 0 V for the diffusion-limited reduction of FcTMA^{2+} back to FcTMA$^+$. The two QRCEs were at ground. A schematic of this configuration is shown in Figure 2A. The resulting generation voltammogram and collection response are shown in Figure 2B, where the potential refers to that of the generator electrode. The diffusion-limited collection efficiency, defined as the ratio of the collection current to generation current, was ca. 80 % in this case, which is higher than the collection efficiencies previously reported for dual carbon probes in a bulk solution.[30] The droplet configuration confines the diffusional mass transport to the meniscus, and as a result a large proportion of the FcTMA^{2+} produced at the generator electrode reaches

8

the collector electrode where it is reduced back to FcTMA$^+$ (with only a small amount escaping up the two open barrels of the probe). Note that the estimation of collection efficiency in this way does not account for the oxidized and reduced forms of the redox mediator (FcTMA$^{+/2+}$) having slightly different diffusion coefficients,[35] although this would only have a minor effect and, in any case, does not influence the steady-state current ratio under quantitative (100%) collection. The regeneration of FcTMA$^+$ at the collector electrode increases its flux to the generator electrode, evident as an increase in the generation current (compared to the response of the individual electrode with the second carbon electrode unconnected; see Figure 2B).

In subsequent experiments, a quad-probe was mounted onto a piezo-electric positioner and was brought close to a gold electrode to bring the meniscus into surface contact. The area of the gold surface wetted by the meniscus forms a third working electrode (Figure 2C). LSVs were recorded at the substrate electrode for the oxidation of FcTMA$^+$, while the two carbon electrodes were disconnected, and the QRCEs were held at ground. This configuration is similar to that of SECCM and the typical voltammetric response shown as the black dotted line in Figure 2D is that of steady-state diffusion.[34]

A full five electrode configuration was then used with the substrate acting as the generator electrode and the two carbon electrodes in the probe as the collector electrodes (substrate generation/ tip-tip collection mode, by analogy to SECM[6,36]). A schematic of this configuration is shown in Figure 2C. Figure 2D shows an LSV recorded for the oxidation of FcTMA$^+$ to FcTMA^{2+} at the substrate and the collection of FcTMA^{2+} at the two tip electrodes. Both the generation current and the collection currents showed a sigmoidal shape as a function of the generator electrode potential. Notably the generation current was approximately three times larger with the collector electrodes switched on than without. This increase in generation current is due to the regeneration of FcTMA$^+$ at the collector

electrodes which enhances the flux of $FcTMA^+$ to the generator electrode. Individual collection efficiencies of ca. 76 % and ca. 23% were observed for the two carbon electrodes. The variation in collection efficiencies between individual electrodes within the quad-probe can be attributed to the differences in size of the electrodes coupled with the differences in electrode recession and different probe to surface distance.[30] Importantly, the total collection efficiency of ca. 99% observed for the probe in substrate generation/tip-tip collection means that practically all the $FcTMA^{2+}$ generated at the substrate was collected at the probe electrodes. Although the two carbon electrodes in the probes are not identical, as reflected by differences in their collection efficiencies, it is still possible to realize complete collection of the substrate-generated product. At the next level, we have outlined elsewhere that deeper knowledge of the geometry of dual carbon probe electrodes and methods for characterization (e.g. via collection efficiencies) can open up detailed finite element simulations of mass transport to individual electrodes, if required.[30]

Electrochemical Imaging. The ion current between the two QRCEs was used as a signal to detect the engagement of the meniscus with the surface, allowing the probe to be laterally scanned across a surface following the contours of the surface as in SECCM.[20]

To test the suitability of this quad-probe for continuous surface electrochemical measurements in an aqueous environment, lines scans profiles were obtained across a gold band substrate on glass, using an ion current based feedback control similar to SECCM[13] (see Supporting Information, Section 4 for typical data and discussion).

In order to demonstrate the feasibility of using quad-probes for high resolution electrochemical imaging with non-aqueous electrolytes, electrochemical activity maps of an individual SWNT on an insulating (Si/SiO_2) substrate were recorded by operating in a surface generation/tip-tip collection configuration using the $FcTMA^{+/2+}$ redox couple in a RTIL

(Figure 3A). A potential difference of 0.1 V was applied between the two QRCEs in the probe ($V_3 = -0.05$ V, $V_4 = 0.05$ V) to induce an ion current between the QRCEs for positional control (see Supporting Information, Section 5). Electrical connection to the SWNT was established through a palladium side contact with the potential (V_5) held at 0.45 V while keeping the potential of the two carbon electrodes in the quad-probe (V_1 and V_2) at 0 V, allowing the oxidation of FcTMA$^+$ to FcTMA^{2+} at the SWNT in contact with the meniscus along with the diffusion-limited collection of FcTMA^{2+} at the two probe electrodes as outlined in the diagram in Figure 3A. The electrochemical images were recorded as a series of lines scans over a scan area of 15 µm by 15 µm, with a line scan every 2 µm at a scan rate of 1 µm/s.

Amperometric maps recorded during a typical surface generation/tip-tip collection scan are shown in Figure 3 (Panels B to D) including the line profiles of electrochemical currents recorded at the SWNT substrate (Panel B and C), and generation current, individual electrode collection currents and overall collection efficiency maps (Panel D), respectively. No current was observed at either the probe electrodes or at the substrate while the tip was scanning over the insulating (Si/SiO$_2$) substrate as no FcTMA^{2+} could be produced at the surface. As the probe encountered the SWNT, the generation current at the SWNT gradually increased, reaching a maximum value when the center of the probe was directly over the SWNT. This is a consequence of the large length of SWNT in contact with the meniscus and the maximum recycling of the FcTMA^{2+} into FcTMA$^+$ by the probe electrodes, since the SWNT is located between both electrodes. An average generation current of ca. 2.3 ± 0.5 pA was recorded at the SWNT at this maximum point. Average collection currents of ca. 1.5 ± 0.3 pA at electrode 1 and 0.65 ± 0.2 pA at electrode 2 were detected while the meniscus was scanning across the SWNT, with an overall collection efficiency of ca. 92 ± 8 %.

The 'width' of the electroactive area in both the generation current and collection efficiency maps as the quad-probe traverses the SWNT (ca. < 5 μm) gives a good guide as to the meniscus size, and is similar to that of the probe employed. This highlights that multifunctional and electrochemical imaging can be carried out with these new quad-probes with a spatial resolution similar to the probe size.

Transient spot measurements: Electrostatic charged insulators and pH evolution. A key advantage of the droplet based quad-probe is the capability to measure the electrochemical current at the tip working electrodes due to substrate-generated products (including at insulators) upon initial meniscus contact. As an example, we measured the excess negative charge present on a Teflon surface after contact electrification.[37] Teflon surfaces were negatively charged by rubbing them with poly(methyl methacrylate) (PMMA). The resulting charge has been shown to drive the reduction of metals ions to metals as well as several redox mediators.[38] Herein, we used the $Ru(NH_3)_6^{3+/2+}$ redox couple to electrochemically detect the amount of negative charge present on a Teflon surface following contact electrification as illustrated in Figure 4A.

The probe, containing aqueous electrolyte with 0.1 mM $Ru(NH_3)_6^{3+}$, and with the carbon electrodes held at 0.0 V (Vs Ag/AgCl QRCE) to detect any $Ru(NH_3)_6^{2+}$ that might be produced, was approached towards the charged Teflon surface (using i_{AC} feedback), halted immediately following initial meniscus contact, and held for ca. 15 s at the substrate. Figure 4B shows the electrochemical current over time throughout this entire process. A transient electrochemical current was observed immediately following meniscus contact, that is due to the flux of $Ru(NH_3)_6^{2+}$ from the charged Teflon surface, that is oxidised back to $Ru(NH_3)_6^{3+}$ at the carbon electrodes. From the charge of the current transient recorded at the tip electrode (black line, Figure 4B), the charge at the Teflon substrate was found to be ca. 14 nC cm^{-2} (3 μm diameter meniscus footprint), consistent with the values found using bulk measurements

using a Faraday cup.[39] Control measurements at an uncharged Teflon surface (red line, Figure 4B) did not show any detectable change in the electrochemical current upon contact. The local point measurements shown here could be extended in the future for surface mapping of charged insulators, particularly as charge heterogeneities might be expected across the surface as implied from heterogeneous metal deposits.[39] Technologically, such measurements could be valuable as Teflon substrates that exhibit micro-nanoscale surface roughness are being explored for energy harvesting with impinging water droplets.[40]

In addition, the carbon working electrodes were functionalized with hydrous iridium oxide (IrOx) to create a pH responsive electrode[31] to follow the local pH change during the initial dissolution of a *pristine* calcite crystal surface. For this measurement, a functionalized quad-probe was filled with 10 mM KCl solution (pH 6.8) and brought into contact with a freshly cleaved calcite surface to form a thin layer electrochemical cell between the probe and crystal surface (Figure 4C). Instantaneous meniscus contact (using i_{AC} feedback (Figure 4D)) prompted dissolution of calcite causing the pH to increase. The pH response of these probes is fast and the transient is not associated with the electrode response time, but rather highlights the surface kinetics, for example the nucleation and expansion of nanopits,[41] to create a surface where the dissolution attains a steady-state (plateau of pH). pH responses of this type could be analyzed to reveal the kinetics of dissolution with further study. Figure 4D shows that a pH change (ca. 0.08 pH units) at the surface was detected following contact and highlights the significant prospect of a quad-barrel approach in crystal dissolution studies where it is challenging to measure such transient and subtle processes at *pristine surfaces* (rather than partially reactive as with other techniques[41]) with sub-second resolution. Additionally, in cases where surface fouling is a concern, such as in corrosion and other processes, this approach of transient meniscus contact offers tremendous opportunity for functional mapping.

CONCLUSIONS

The rapid fabrication of multifunctional *quad-probes* has been described. Merging key features of SECM and SECCM, these probes incorporate two working electrodes immersed in a liquid meniscus that can be operated in various generation-collection modes. As an imaging tool, the quad-probe enables localized high resolution electrochemical imaging of surfaces and interfaces, and is particularly attractive given the high collection efficiencies inherent in this configuration.

The capability of these probes for the localized electrochemical investigation of surfaces was demonstrated by employing them for electrochemical imaging of an individual SWNT substrate. Moreover, the suitability of these probes for electrochemical measurements in non-aqueous environments was also demonstrated by using a RTIL as the supporting electrolyte. This is particularly noteworthy, as studies of RTILs with SECM are recognized to be difficult with the low diffusion coefficients and often large differences of the diffusion coefficients of oxidized and reduced species, making steady-state feedback measurements difficult with μm sized probes[43-45] and − hitherto - necessitating the use of extremely high redox concentrations with smaller probes.[46] Further, the capability of these probes for transient current measurements on insulating and reactive surfaces was demonstrated. This aspect opens up the prospect of surface titrations and adsorption/modification measurements on a wide range of surfaces.

In general quad-probes permit simultaneous detection of multiple targets in a confined droplet, which may allow many interesting and difficult substrates to be investigated in the future. Moreover, these probes could easily be modified to integrate with other electrochemical techniques such as scanning ion conductance microscopy (SICM)[29] where multiple electrodes and detection of multiple species could be highly valuable. In this

context, as well as for meniscus based imaging, it should be mentioned that the carbon electrodes can be sensitized to expand the range of species that can be detected amperometrically[47] and potentiometrically.[31] Beyond electrochemistry, micropipettes and nanopipettes find increasing use in analytical science from fluidic systems to electrospray techniques, and the ability to incorporate multiple sensor electrodes into such devices could be beneficial in future applications.
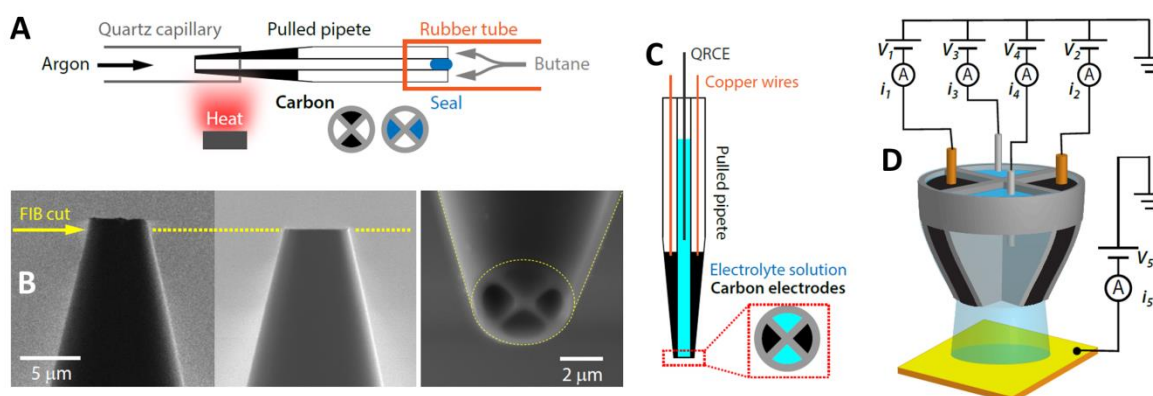
Acknowledgements

Figure 1. (A) Schematic of the carbon deposition step for the fabrication of a quad-probe. Two diagonally opposite barrels were closed by using *Blu-Tack* (Bostik, UK) and butane was passed through the other two barrels. The tip of the pipet was heated with a butane torch under an argon atmosphere to pyrolytically deposit carbon from the butane.[29-31] **(B)** FIB-SEM micrograph (side view) of the quad-probe before (left) and after (middle) FIB cutting. On the right is an SEM micrograph of the end of a typical quad-probe showing carbon electrodes (top and bottom) and open barrels (left and right). **(C)** Schematic of the fabricated quad-probe. **(D)** Schematic of the five electrode configuration: two carbon working electrodes in the barrel of the probe, and two open barrels filled with electrolyte and AgCl coated Ag wire QRCEs, and a substrate electrode. The voltage of each electrode, with respect to ground, was controlled separately (V_{1-5}), and the currents at each electrode (i_{1-5}) were recorded separately.
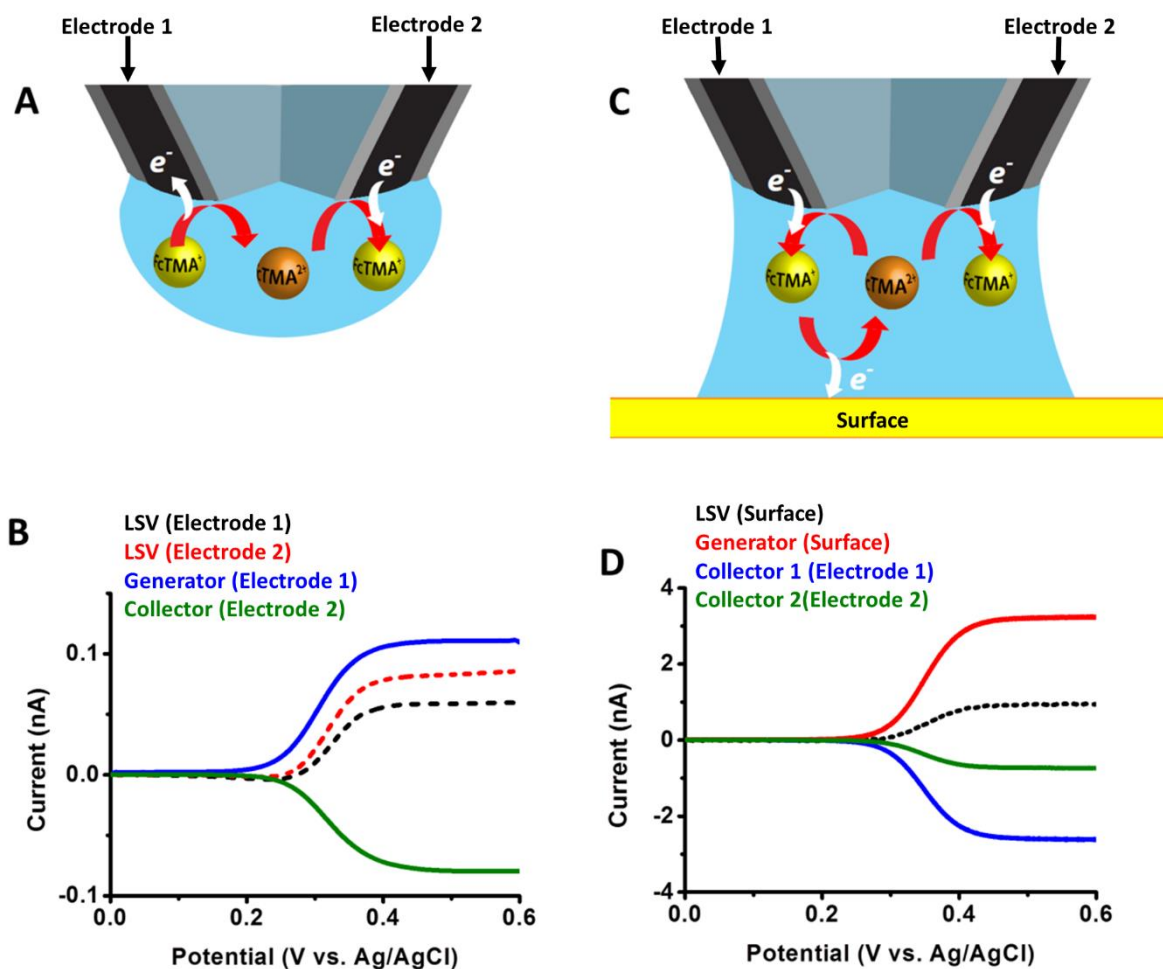
Figure 2. (**A**) Schematic of the quad-probe in tip generation-tip collection mode, with the probe away from a surface and FcTMA$^{+/2+}$ couple as the redox mediator. One electrode (left) oxidizes FcTMA^{+} to FcTMA^{2+}, while the other (right) reduces FcTMA^{2+} to FcTMA^{+}. The QRCES in the open channels (not shown) act as the reference/counter electrodes. (**B**) LSVs for the oxidation of FcTMA^{+} to FcTMA^{2+} at two electrodes in the quad-probe. Each was swept with the other working electrode unconnected (black and red dotted lines) and voltammetric responses for the FcTMA$^{+/2+}$ couple as the potential of the generator electrode was swept between 0 V and 0.6 V and the collector electrode current was held constant at 0 V for the same probe (blue and green solid lines) were also shown. (**C**) Schematic of the quad-probe in substrate generation/tip-tip collection mode. The substrate electrode oxidizes

17

FcTMA$^+$ to FcTMA^{2+}, while the probe electrode reduces FcTMA^{2+} to FcTMA$^+$. The QRCEs in the open barrels in the probe act as the reference/counter electrodes. **(D)** LSVs for the oxidation of FcTMA$^+$ to FcTMA^{2+} at the substrate while the other electrodes were unconnected (black dotted line) and LSVs for the generation and collection currents in surface generation/tip-tip collection mode for FcTMA$^{+/2+}$ couple as the redox mediator for the same probe. The potential of the generator electrode was swept from 0 V to 0.6 V and the potential of the collector electrodes was held constant at 0 V**.**
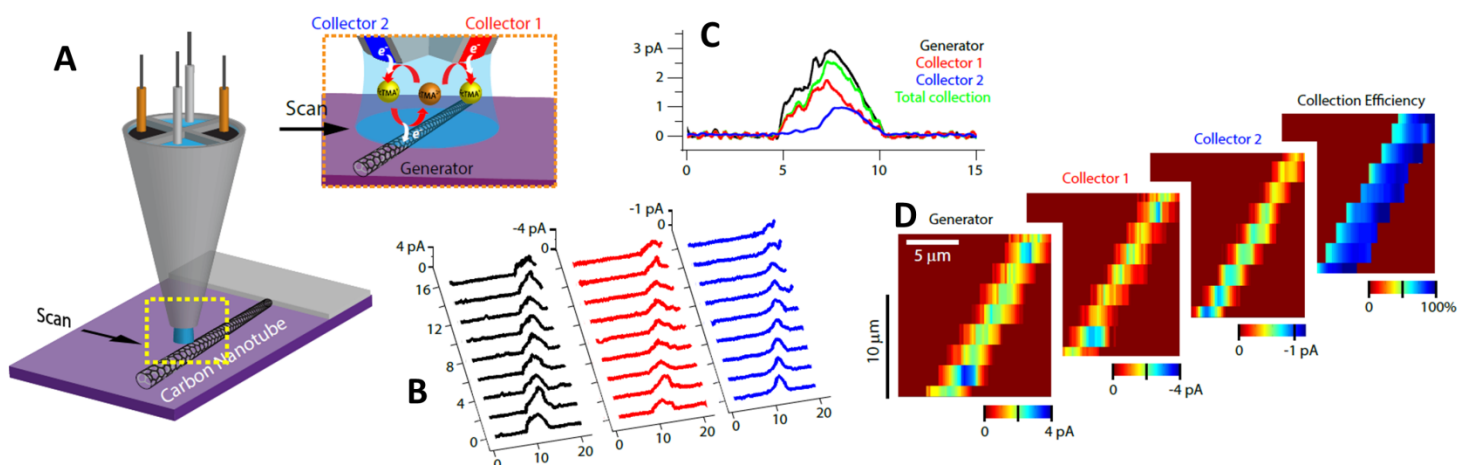
Figure 3. (A) Schematic of imaging in surface generation/ tip-tip collection mode with a five electrode configuration. The substrate (SWNT) was held at a potential that generated FcTMA^{2+}, while the two carbon electrodes in the probe were held at a potential to collect any FcTMA^{2+} produced. **(B)** Line profiles of generation (black), and collection (red and blue) currents recorded as the probe was scanned over a SWNT. **(C)** Current profiles (magnitude) recorded during a single line scan illustrating the induction of electrochemical currents at each electrode, as the meniscus passed over the SWNT. **(D)** Generator, collector 1, collector 2 and collection efficiency maps recorded on a SWNT.
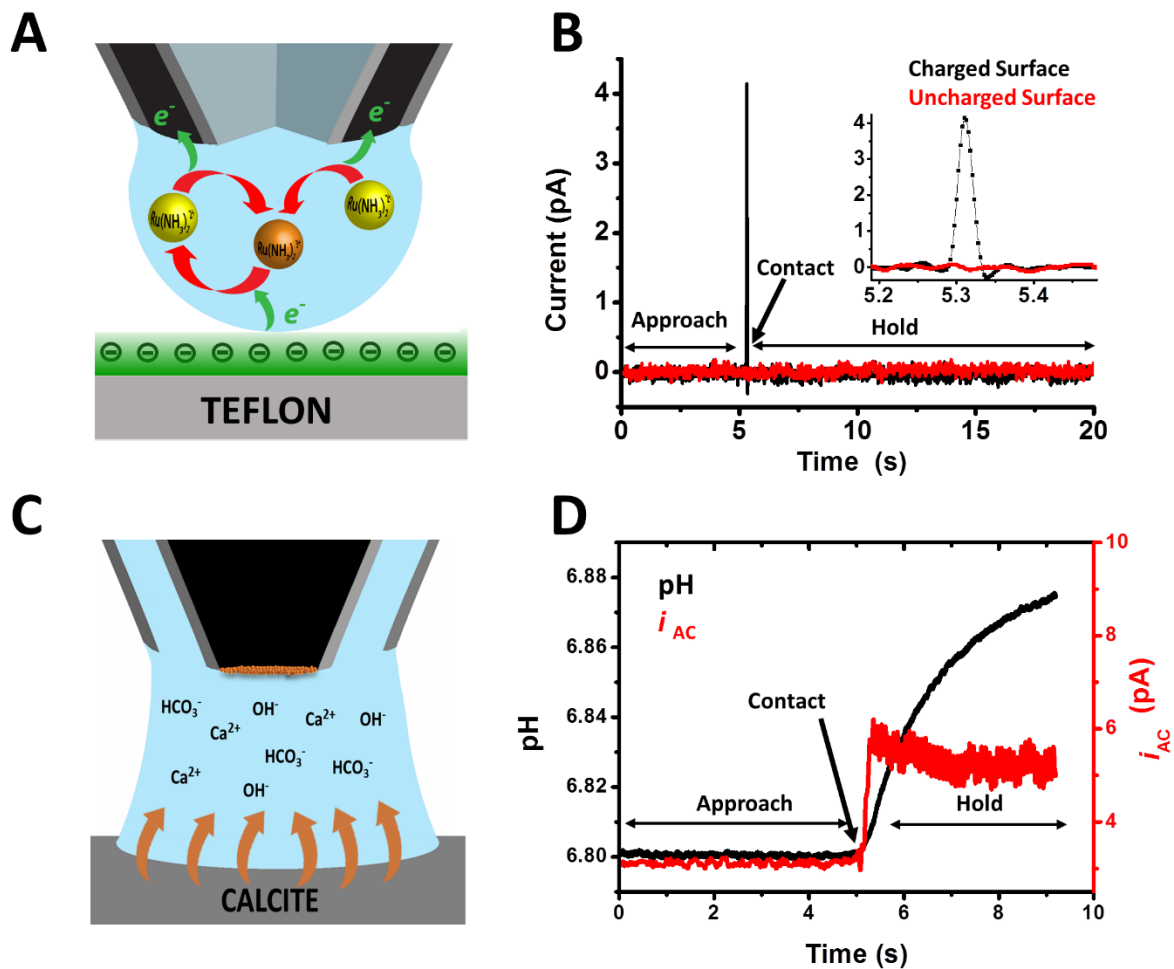
Figure 4. (A) Schematic of electrostatic electrochemistry using a $Ru(NH_3)_6{}^{3+}$/ $Ru(NH_3)_6{}^{2+}$ redox couple at a negatively charged Teflon surface. The negative surface charge on the Teflon reduces $Ru(NH_3)_6{}^{3+}$ to $Ru(NH_3)_6{}^{2+}$, which then diffuses towards the probe electrodes where it is oxidized (and measured) to $Ru(NH_3)_6{}^{3+}$. The QRCEs in the open channels (not shown) act as the reference/counter electrodes. **(B)** Approach curves showing the electrochemical current measured at the quad-probe working electrodes upon contact with a negatively charged Teflon surface (black line) and an uncharged Teflon surface (red line). (Inset: zoom-in showing individual data points during transient current measurement) **(C)** Schematic of the dissolution of calcite when the quad-probe meniscus is in contact with the calcite surface. The open circuit potential between the pH electrode and one the QRCEs in

the open channels (held at 0 V with respect to ground, not shown) was measured using a home-built voltage follower.[31] **(D)** pH and i_{AC} recorded at the quad-probe during approach to a pristine calcite surface showing feedback control (i_{AC}) and an increase in pH after the meniscus came into contact with the calcite surface.

References

(1) Kosmulski, M. *Chemical properties of material surfaces*; Marcel Dekker: NY, 2001.

(2) Wang, G.; Zhang, L.; Zhang, *J. Chem. Soc. Rev.* **2012**, *41*,797-828.

(3) Mauzeroll, J.; Bard, A. J. *Proc. Natl Acad. Sci.* USA **2004**, *101*, 7862-7867.

(4) Amemiya, S.; Bard, A. J. *Anal. Chem.* **2000**, *72*, 4940-4948.

(5) Aaronson, B. D. B.; Lai, S. C. S.; Unwin, P. R. *Langmuir* **2014**, *30*, 1915-1919.

(6) Bard, A. J.; Mirkin, M. V. (eds.) *Scanning electrochemical microscopy*; 2nd ed.; CRC Press: Boca Raton, FL., 2012.

(7) Bard, A. J.; Fan, F. R. F.; Kwak, J.; Lev, O. A. *Anal. Chem.* **1989**, *61*,132-138.

(8) Bard, A. J.; Denuault, G.; Lee, C.; Mandler, D.; Wipf, D. O. *Acc. Chem. Res.* **1990**, *23*, 357-363.

(9) Lohrengel, M. M.; Moehring, A.; Pilaski, M. Fresen. J. *Anal. Chem.* **2000**, *3*67, 334-339.

(10) Gasiorowski, J.; Kollender, J. P.; Hingerl, K.; Sariciftci, N. S.; Mardare, A. I.; Hassel, A. W. *Phys. Chem. Chem. Phys.* **2014**, *16*, 3739-3748.

(11) Clausmeyer, J.; Henig, J.; Schuhmann, W.; Plumere, N. *Chemphyschem* **2014**, *15*, 151-156.

(12) Amemiya, S.; Bard, A. J.; Fan, F.-R. F.; Mirkin, M. V.; Unwin, P. R. *Annu. Rev. Anal. Chem.* **2008**, *1*, 95-131.

(13) Zhou, J.; Zu, Y.; Bard, A. J. *J. Electroanal. Chem.* **2000**, *491*, 22– 29.

(14) Kranz, C. *Analyst* **2014**, *139*, 336-352.

(15) Lohrengel, M. M.; Moehring, A.; Pilaski, M. *Electrochim. Acta* **2001**, *47*, 137-141.

(16) Arjmand, F.; Adriaens, A. *J. Solid State Electr.* **2014**, *18*, 1779-1788.

(17) Ebejer, N.; Güell, A. G.; Lai, S. C. S.; McKelvey, K.; Snowden, M. E.; Unwin, P. R. *Annu. Rev. Anal. Chem.* **2013**, *6*, 329-351.

(18) Cortes-Salazar, F.; Momotenko, D.; Girault, H. H.; Lesch, A.; Wittstock, G. *Anal. Chem.* **2011**, 83, 1493-1499.

(19) Williams, C. G.; Edwards, M. A.; Colley, A. L.; Macpherson, J. V.; Unwin, P. R. *Anal. Chem.* **2009**, *81*, 2486-2495.

(20) Ebejer, N.; Schnippering, M.; Colburn, A. W.; Edwards, M. A.; Unwin, P. R. *Anal. Chem.* **2010**, *82*, 9141-9145.

(21) Rodolfa, K. T.; Bruckbauer, A.; Zhou, D. J.; Korchev, Y. E.; Klenerman, D. *Angew. Chem. Int. Ed.* **2005**, *44*, 6854-6859.

(22) Rodolfa, K. T.; Bruckbauer, A.; Zhou, D. J.; Schevchuk, A. I.; Korchev, Y. E.; Klenerman, D. *Nano Letters* **2006**, *6*, 252-257.

(23) O'Connell, M. A.; Snowden, M. E.; McKelvey, K.; Gayet, F.; Shirley, I.; Haddleton, D. M.; Unwin, P. R. *Langmuir* **2014**, *30*, 10011–10018.

(24) Güell, A. G.; Ebejer, N.; Snowden, M. E.; Macpherson, J. V.; Unwin, P. R. *J. Am. Chem. Soc.* **2012**, *134*, 7258-7261.

(25) Güell, A. G.; Meadows, K. E.; Dudin, P. V.; Ebejer, N.; Macpherson, J. V.; Unwin, P. R. *Nano Letters* **2014**, *14*, 220-224.

(26) Cortes-Salazar, F.; Lesch, A.; Momotenko, D.; Busnel, J.-M.; Wittstock, G.; Girault, H. H. *Anal. Methods* **2010**, *2*, 817-823.

(27) Momotenko, D.; Cortes-Salazar, F.; Lesch, A.; Wittstock, G.; Girault, H. H. *Anal. Chem.* **2011**, *83*, 5275-5282.

(28) Momotenko, D.; Qiao, L.; Cortes-Salazar, F.; Lesch, A.; Wittstock, G.; Girault, H. H. *Anal. Chem.* **2012**, *84*, 6630-6637.

(29) Takahashi, Y.; Shevchuk, A. I.; Novak, P.; Zhang, Y.; Ebejer, N.; Macpherson, J. V.; Unwin, P. R.; Pollard, A. J.; Roy, D.; Clifford, C. A.; Shiku, H.; Matsue, T.; Klenerman, D.; Korchev, Y. E. *Angew. Chem. Int. Ed.* **2011**, *50*, 9638-9642.

(30) McKelvey, K.; Nadappuram, B. P.; Actis, P.; Takahashi, Y.; Korchev, Y. E.; Matsue, T.; Robinson, C.; Unwin, P. R. *Anal. Chem.* **2013**, *85*, 7519-7526.

(31) Nadappuram, B. P.; McKelvey, K.; Al Botros, R.; Colburn, A. W.; Unwin, P. R. *Anal. Chem.* **2013**, *85*, 8070-8074..

(32) Thakar, R.; Weber, A. E.; Morris, C. A.; Baker, L. A. *Analyst* **2013**, *138*, 5973-5982.

(33) Macpherson, J. V.; Simjee, N.; Unwin, P. R. *Electrochim. Acta* **2001**, *47*, 29-45.

(34) Snowden, M. E.; Güell, A. G.; Lai, S. C. S.; McKelvey, K.; Ebejer, N.; O'Connell, M. A.; Colburn, A. W.; Unwin, P. R. *Anal. Chem.* **2012**, *84*, 2483-2491.

(35) Lazenby, R. A.; McKelvey, K.; Peruffo, M.; Baghdadi, M.; Unwin, P. R. *J. Solid State Electr.* **2013**, *17*, 2979-2987.

(36) Sun, P.; Laforge, F. O.; Mirkin, M. V. *Phys. Chem. Chem. Phys.* **2007**, *9*, 802-823.

(37) Liu, C.; Bard, A. J. *Nat. Mater.* **2008**, 7,506-509.

(38) Liu, C.; Bard, A. J. *J. Am. Chem. Soc.* **2009**, *131*, 6397-6401.

(39) Baytekin, B.; Baytekin, T. H.; Grzybowski, B. A. *J. Am. Chem. Soc.* **2012**, *134*, 7223-7226.

(40) Lin, Z.; Cheng, G.; Lee, S., Pradel, K. C.; Wang Z. L. *Adv. Mater.* **2014**, *26*, 4690-4696.

(41) Jones, C. E.; Unwin, P. R.; Macpherson, J. V. *ChemPhysChem* **2003**, *4*, 139-146.

(42) Kinnear, S. L.; McKelvey, K.; Snowden, M. E.; Peruffo, M.; Unwin, P. R. *Langmuir* **2013**, *29*, 15565-15572.

(43) Martin, R. D.; Unwin, P. R. *J. Electroanal. Chem.* **1997**, *439*, 123-136.

(44) Ghilane, J.; Lagrost, C.; Hapiot, P. *Anal. Chem.* **2007**, *79*, 7383-7391.

(45) Carano, M.; Bond, A. M. *Aust. J. Chem.* **2007**, *60*, 29-34.

(45) Laforge, F. O.; Velmurugan, J.; Wang, Y.; Mirkin, M. V. *Anal. Chem.* **2009**, *81*, 3143-3150.

 (47) Actis, P.; Tokar, S.; Clausmeyer, J.; Babakinejad, B.; Mikhaleva, S.; Cornut, R.; Takahashi, Y.; Cordoba, A. L.; Novak, P.; Shevchuck, A. I.; Dougan, J. A.; Kazarian, S. G.; Gorelkin, P. V.; Erofeev, A. S.; Yaminsky, I. V.; Unwin, P. R.; Schuhmann, W.; Klenerman, D.; Rusakov, D. A.; Sviderskaya, E. V.; Korchev, Y. E. *ACS Nano* **2014**, *8*, 875-884.

For TOC Only